Video Article

Second Harmonic Generation Signals in Rabbit Sclera As a Tool for Evaluation of Therapeutic Tissue Cross-linking (TXL) for Myopia

Mariya Zyablitskaya[1], E. Laura Munteanu[2], Takayuki Nagasaki[1], David C. Paik[1]

[1]Department of Ophthalmology, Columbia University College of Physicians and Surgeons

[2]Confocal and Specialized Microscopy Shared Resource, Herbert Irving Comprehensive Cancer Center, Columbia University

Correspondence to: David C. Paik at dcp14@cumc.columbia.edu

URL: https://www.jove.com/video/56385
DOI: doi:10.3791/56385

Keywords: Medicine, Issue 131, Sodium hydroxymethylglycinate, tissue cross-linking, high myopia, sclera, second harmonic generation signal, thermal denaturation temperature, differential scanning calorimetry, rabbit eyes

Date Published: 1/6/2018

Citation: Zyablitskaya, M., Munteanu, E.L., Nagasaki, T., Paik, D.C. Second Harmonic Generation Signals in Rabbit Sclera As a Tool for Evaluation of Therapeutic Tissue Cross-linking (TXL) for Myopia. *J. Vis. Exp.* (131), e56385, doi:10.3791/56385 (2018).

Abstract

Methods to strengthen tissue by introducing chemical bonds (non-enzymatic cross-linking) into structural proteins (fibrillar collagens) for therapy include photochemical cross-linking and tissue cross-linking (TXL) methods. Such methods for inducing mechanical tissue property changes are being employed to the cornea in corneal thinning (mechanically weakened) disorders such as keratoconus as well as the sclera in progressive myopia, where thinning and weakening of the posterior sclera occurs and likely contributes to axial elongation. The primary target proteins for such tissue strengthening are fibrillar collagens which constitute the great majority of dry weight proteins in the cornea and sclera. Fortuitously, fibrillar collagens are the main source of second harmonic generation signals in the tissue extracellular space. Therefore, modifications of the collagen proteins, such as those induced through cross-linking therapies, could potentially be detected and quantitated through the use of second harmonic generation microscopy (SHGM). Monitoring SHGM signals through the use of a laser scanning microscopy system coupled with an infrared excitation light source is an exciting modern imaging method that is enjoying widespread usage in the biomedical sciences. Thus, the present study was undertaken in order to evaluate the use of SHGM microscopy as a means to measure induced cross-linking effects in *ex vivo* rabbit sclera, following an injection of a chemical cross-linking agent into the sub-Tenon's space (sT), an injection approach that is standard practice for causing ocular anesthesia during ophthalmologic clinical procedures. The chemical cross-linking agent, sodium hydroxymethylglycinate (SMG), is from a class of cosmetic preservatives known as formaldehyde releasing agents (FARs). Scleral changes following reaction with SMG resulted in increases in SHG signals and correlated with shifts in thermal denaturation temperature, a standard method for evaluating induced tissue cross-linking effects.

Video Link

The video component of this article can be found at https://www.jove.com/video/56385/

Introduction

Progressive myopia is postulated to be treatable through non-enzymatic scleral cross-linking (photochemical and/or chemical), which makes sense given that blocking collagen enzymatic cross-linking can increase experimental form deprivation (FD)-induced myopia[1]. Elsheikh and Phillips[2] recently discussed the feasibility and potential of using standard ultraviolet-A irradiation (UVA)-riboflavin mediated photochemical cross-linking (also known as the Dresden protocol), abbreviated here as (riboflavin CXL) for posterior scleral stabilization to halt axial elongation in myopia. This photochemical method has been successfully used for treating destabilization of the anterior globe surface (*i.e.*, the bulging cornea) seen in keratoconus and post-LASIK keratectasia. However, application of this CXL protocol for the sclera is hindered by issues related to difficulties in accessing the posterior sclera with an ultraviolet (UV) light source, as well as the need to modify a much greater tissue surface area. That being said, the CXL approach has been used to halt axial elongation in visually form deprived rabbits (by tarsorrhaphy), although multiple regions of posterior sclera required multiple separate irradiation zones in that study[3]. By contrast, injection of a chemical stabilizing agent (*i.e.*, cross-linking agent) via the sT space could represent a simpler way to modify the posterior sclera, avoiding the need for introducing a UV light source. This injection technique is well known as a useful way of inducing ocular anesthesia during ophthalmologic procedures such as cataract surgery[4,5,6]. Wollensak[7] has described previously the use of an sT injection using glyceraldehyde (a chemical cross-linking agent similar in concept to the formaldehyde releasing agents (FARs) described in this study) to stiffen the rabbit sclera and genipin has been shown to limit axial length in FD guinea pigs[8,9]. These investigators have demonstrated a clear advantage of using a soluble chemical agent over the photochemical CXL technique. Thus, scleral cross-linking using an injectable chemical agent of some type, including the FARs (*i.e.*, TXL)[10], could provide a feasible treatment method to halt the progression of scleral elongation seen in myopia.

In the protocols presented here, we use a chemical cross-linking solution of sodium hydroxymethylglycinate (SMG), delivered via sT injection to the sclera of cadaveric rabbit eyes. We have implemented similar protocols previously for topical chemical cross-linking in the cornea. Notably in those previously reported studies, concentration dependent cross-linking effects could be obtained using SMG, with an effect range spanning well above that achievable with photochemical CXL as determined by thermal denaturation analysis[11].

Here we describe protocols to assess the cross-linking effect of SMG delivered via sT injections to scleral tissue, thermal denaturation using Differential Scanning Calorimetry (DSC), and Second Harmonic Generation Microscopy (SHGM).

Using differential scanning calorimetry (DSC), also known as thermal analysis, a thermal denaturation transition is measured, which for scleral tissue is predominately guided by the properties of the fibrillar collagens, since they constitute the bulk majority of protein. This method evaluates the stability of collagen molecular structure and the cross-linked bonds that stabilize the collagen fibrils, the principal tertiary protein structure. During heating in the DSC, a critical transition temperature is achieved that results in denaturation of the collagen molecule, resulting in uncoiling of the triple helix, a process that forms what is commonly known as gelatin. This thermal denaturation disrupts hydrogen bonds along the collagen molecule and can be shifted to higher temperatures through induced cross-linking methods[12,13]. This method has been used for many decades, particularly in the biomaterials industry and for processes that include leather-making. However, this method requires extraction of the sclera tissue and therefore can only be useful as an *ex vivo* technique.

Second-harmonic generation microscopy (SHGM) is based on the non-linear optical properties of particular materials, with non-centrosymmetric molecular environments. In such materials, intense light, for example light produced by lasers, generates SHG signals, in which the incident light is doubled in frequency. Biological materials that are known to create SHG signals are collagen, microtubules, and muscle myosin. For example, collagen excited with an infrared light of 860 nm wavelength will emit an SHG signal in the visible range with 430 nm wavelength. Second harmonic generation (SHG) signal imaging is a promising method for evaluating therapeutic collagen cross-linking. It has been known for more than 30 years that collagen fibrils in tissues emit SHG signals[14]. However, only recently could high resolution images be obtained[15] in a variety of tissues, including tendon[16], skin, cartilage[17], blood vessels[18], and in collagen gels[19].

Based on this knowledge, this study evaluates the SHG signal changes induced in the sclera through SMG chemically induced cross-linking of collagen. The results indicate that SMG modification of the sclera increases the SHG signals produced from tissue collagen fiber bundles (the higher order quaternary structure comprised of collagen fibrils) and also produces a structural morphologic change in the collagen fiber network, reflected in fiber bundle "straightening."

Protocol

All procedures were performed using cadaveric rabbit eyes within intact outbred rabbit heads. All Institutional and National guidelines for the care and use of laboratory animals were followed.

1. Preparation of Solutions

1. SMG preparation for TXL:
    1. Prepare 1 mL of 0.2 M concentration of sodium bicarbonate solution ($NaHCO_3$) solution using 0.0165g of NaHCO3 powder dissolved in 1 mL of the distilled water.
    2. Dissolve 0.1016 mg of powdered sodium hydroxymethylglycinate (SMG) in 1 mL of the distilled water to get a final concentration of 800 mM SMG. Adjust sodium bicarbonate solution to a final concentration of 0.1 M $NaHCO_3$ and 400 mM SMG. Concentrations of SMG depending on the cross-linking effect desired. In the protocol described here we used 40, 100, and 400 mM SMG.

2. SubTenon's Injection for TXL using SMG

1. Fill two 1 mL insulin syringes (25G needles) with 400 µL control and SMG solution, respectively.
2. Place the rabbit's head in a profile plane with the help of a cushion. Styrofoam or a paper stack can be used to fix the head in an optimal position.
3. Retract the eyelids with a pediatric eye speculum.
4. Measure the initial intraocular pressure (IOP) using an applanation tonometry device.
5. Mark the site of intended injection on the upper middle part of the limbus with a tissue marker.
6. Retract the conjunctiva surrounding the site of injection with a conjunctival forceps (or any forceps with serrated round tip) and insert the needle through the conjunctiva, entering Tenon's capsule just slightly beyond the marked limbal site (*i.e.*, 2-3 mm from the limbus). A small incision in the conjunctiva can also be made with iris scissors in order to facilitate the passage of the needle through Tenon's capsule.
7. Once within Tenon's capsule, make sure that the needle is freely mobile by moving it side-to-side. During this time, the globe should not move. This confirms proper placement of the needle above the sclera in the sub-Tenon's (sT) space.
8. Inject the solution from the syringe and discard the needle. Immediately following injection, the fluid will accumulate in the sT space creating an anterior bulge seen through the conjunctiva (*i.e.*, chemosis).
9. Repeat the IOP measurement in order to confirm that it did not change due to an inadvertent perforation of the globe.
10. Remove the lid speculum, and perform digital massage through the closed eyelids for about 2-3 min.
11. Leave the head for an incubation period of 3.5 h (room temperature = 18 °C), prior to moving to the next step.

3. Tissue Preparation

1. Retract the eyelids using the eyelid speculum in order to optimize access to the globe. Select the optimally sized speculum according to the size of the eye.
2. Separate the conjunctiva surrounding the limbus. If it has already been incised near the site of injection, circumferentially expand the borders so it would contain an inoculum size of approximately 1x1 cm.
3. Cut the extra-ocular muscles at their sites of scleral insertion.
4. Elevate the eyeball with forceps, pushing it from the posterior side. This provides access to the posterior globe and will facilitate cutting of the optic nerve with ophthalmic artery and vein located near the posterior pole of the globe.

5. Cut out the corneoscleral complex, with the outer border including the marked injection site. The stain should still be visible on the remaining part of the sclera.
6. Remove the *corpus vitreus* and all layers attached to the inner side of the sclera by applying traction with tissue forceps.
   NOTE: Further steps depend on the following procedures being performed: 4.-DSC analysis, 5.-SHG microscopy.

4. For Regional DSC Analysis

1. **For the treated eye:** cut out four scleral sectors from the remaining scleral cup with the scissors so that the site of the injection is located in the upper sector and aligned centrally. Cut the remaining 3 sectors from both lateral sides (*i.e.*, nasal and temporal), and the bottom.
   NOTE: the numbering of the sectors (1-4) which are further divided into squares (1-16) is demonstrated in **Figure 1A**.
2. Cut the scleral sectors (1-4) into smaller squares (1-16) of approximately 4 x 4 mm each. Sector 1 should be divided into 9 squares (make the exact site of injection an individual square [square 2]). Divide sectors 2 and 3 into 2 squares each (squares 10-11 and 12-13) and sector 4 into 3 squares (squares 14-16).
3. Assign a number to each square, as shown in **Figure 1A**, in order to localize the distance of the analyzed tissue from the location of the injected area.
4. **For the control eye:** after dividing the tissue into four scleral sectors (similar to the treated tissue) cut out square pieces of tissue from the following locations: 3 squares from the top sector (sector 1), 1 from each side (sectors 2 and 3), and 1 from the bottom sector (sector 4).
5. Scrape off the remaining retinal and choroidal layers and wash twice with fresh PBS each time, leaving the pieces submerged in solution for approximately 10 s at a time.

5. For SHG Imaging

1. Cut the upper part of the sclera using scissors to create a 1 x 1 cm area with the site of injection aligned centrally.
2. Scrape off the remaining retinal and choroid layers and wash twice with fresh PBS each time leaving the pieces in solution for approximately 10 s.
3. Place the tissue in 1 mL tubes filled with PBS solution for transportation to the imaging facility. All the procedures, following the incubation time and beginning with the dissection of the eyeball should be performed within an hour.

6. Microscopy Protocol

NOTE: This protocol for imaging back-scattered SHG signal from collagen of sclera tissue is tailored for the laser scanning microscope.

1. **Microscopy set up**
   1. To maximize the signal and resolution when performing SHG microscopy use an objective lens optimize to transmit infrared light and with a high numerical aperture (NA). Our objective is Nikon Apo LWD 25x/NA1.1 water immersion.
   2. Adjust the correction collar of the lens to match the depth of the sample, in this case that is the thickness of the coverslip, 0.17 millimeters.
   3. Mount the 25x objective lens and add a generous amount of lubricating water-based gel to cover the imaging surface before mounting the sample. The water-based gel will not evaporate during the experiment and hence will maintain image quality.
   4. Place the scleral tissue from a 1 mL tube with PBS without drying between two 25-mm round coverslips (episcleral side down) providing maximal contact between the episclera and the coverslip surface.
      NOTE: The tissue can also be placed uncovered on the coverslip. A good amount of PBS should keep the tissue hydrated during imaging. In this case, add the tissue piece and the PBS after assembling the cellchamber.
   5. Assemble the cell chamber by placing a 25-mm round coverslip, single or in a sandwich technique, on the bottom part of the chamber and screw the top part down in order to create a sealed round chamber. Do not screw down tightly when a top coverslip is used, in order to avoid artificially flattening and damage the tissue.
   6. Mount the cell chamber with the tissue sample on the microscope stage.
   7. Set the microscope for eye view with transmitted light on.
   8. Position the stage and adjust the height of the objective such that the lower surface of the sample is in focus, as determined by bright field inspection through the eye piece.
   9. Turn off all lights except the computer monitor and block as much light from the monitor as possible with aluminum foil sheets draped on the microscope stage. Minimizing any stray light reaching the detectors will ensure low-noise acquisition, as the GaAsP NDD detectors have high sensitivity.
   10. In the Ti Pad panel of the software, check that the lens definition is correct.
   11. In the A1 Compact GUI panel, choose the IR laser for imaging, select the NDD detectors and choose the DAPI channel that is equipped with a 400-450 nm bandpass filter.
   12. In the A1 MP GUI panel, set the wavelength of the infrared laser to 860 nm and open the shutter.
   13. Set laser scanning conditions in the A1 Compact GUI panel as follows. Select: (a) Galvano scanner, (b) Unidirectional scanning, (c) Pixel dwell time 6.2 µs, (d) Frame size 1,024 x 1,024 pixels, (e) Line averaging 2x
       NOTE: The Galvano scanner and unidirectional scanning ensures precise point by point alignment. A size of 1,024 x 1,024 for the full field of view translates into a pixel size of 0.5 µm /pixel. Line averaging will reduce the shot noise in the image.
   14. Set imaging conditions in A1 Compact GUI panel by adjusting laser power and detector gain. Open the Look Up Table panel (LUTs) that displays a histogram of pixel intensity values in the current image. Turn on live imaging in “Find” mode and maximize the detected range of pixel values by adjusting laser power and detector gain. Avoid saturation. Typical values are 2.5% laser power, from a total of 2.35 W at 860 nm, and 100 HV (detector gain).
   15. NOTE: For this setup, the laser power measured with an internal power meter is 5.2 mW. Every time an experiment is performed, re-adjust the laser percentage such that the internal power measurement is constant at 5.2 mW between imaging sessions. Care should

be taken when setting laser power. The Chameleon II laser is a 3 W laser at 800 nm and a 10% or higher power could potentially induce tissue damage.

2. **Image acquisition**
    1. In preview mode, scan the tissue area using the XYZ Overview tool.
    2. Set the imaging to lower resolution (256 x 256 pixels and no line averaging) to speed up the acquisition of images in this mode.
    3. Capture 5 x 5, 3 x 3, or single fields of view to cover the entire surface of the tissue. At each location, before the overview capture, turn on the live "Scan" mode and bring the tissue into focus. Note that different regions of the tissue will have slightly different positions in the axial direction.
    4. Find a flat area where the collagen fibers are seen in the entire field of view and double-click that position in the overview tool to move the stage to that particular location.
    5. Turn on live "Scan" mode, adjust the Z position of the objective such that the bottom plane is in focus and, in the Ti Pad, use the Z drive to move the optical plane 10-15 µm above this bottom layer.
    6. Acquire an image at high resolution with 1,024 x 1,024 pixels and 2x line averaging, using the "Capture" button.
    7. Save the location in the XYZ Overview using the "+" button. This ensures that the same area of tissue is not recaptured.
    8. For each piece of tissue capture 10 images of non-overlapping fields of view.

7. DSC Protocol

Note: Proceed to this step as soon as tissue preparation is complete, for regional DSC analysis, or after tissue imaging when SHGM is performed.

1. Prepare DSC pans, weighed and labeled.
   NOTE: This step should be done before tissue dissection in order to minimize tissue desiccation.
2. Dry each scleral square with an absorbent tissue and lay it flat on the bottom of a DSC pan using toothed forceps.
3. Weigh the pan with the tissue inside and lid crimped and covered to obtain the tissue wet weight (mass of the samples should be in the range of 5 to 11 mg).
   Note: Seal each pan using the crimper before proceeding to the next tissue sample. The pans are hermetically sealed, preventing any water loss prior to thermal analysis.
4. Once the sample is crimped, place it on its designated location on the DSC tray. There should be 6 samples for the control and 16 for the treated eye.
5. Create a method using instrument managing software, specifying the weight of the tissue, and run the thermal analysis using the following parameters: Temperature range of 40 to 80 °C, Heating rate: 1 °C/min, Heat flow: 17.37 mW, Gas (N_2) flow: 19.8 mL/min, Gas pressure: 2.2 bar.
6. Once completed, analyze the data for each sample by extracting the transition temperature peak at which thermal denaturation occurs using the instrument managing software.

8. Image Analysis

1. **SHG Signal**
    1. Select at least 5-10 of the most representative images from each treatment and its control, such that the area of the image is occupied by mostly collagen fibers.
    2. Upload each image in ImageJ software and measure the average pixel intensity by selecting *Analyze*> *Measure* for the active image.
    3. The values extracted are reported as the mean pixel intensity and can also be shown by plotting the histogram of intensities by selecting from the menu *Analyze* > *Histogram*.
    4. Using an Excel sheet, create a table to document all measured data accordingly to the sample ID.
    5. Calculate the mean and standard deviation of pixel intensity for each treatment and control condition.
    6. Using student's t-test, compare differences for all pairwise comparisons of concentrations (*i.e.*, 40 mM SMG vs. 0 and 400 mM SMG vs. 0). [P≤0.05].

2. **Waviness**
    1. Select an image that displays collagen fibers. At least 10 images per sample should be analyzed (including a control sample for each concentration - at least 40 in total).
    2. Open *ImageJ*>*Plugins*> *NeuronJ*. *NeuronJ* requires prior installation.
    3. Upload all imagesby dragging into an opened *NeuronJ* window.
    4. Create tracing lines along the fibers, following the contour of the fibril with the mouse (pen drawing tablets could be used), click M to measure the distance of total fiber length.
    5. Select "Option" to draw a tangential straight line and connect the beginning and the end of the previously drawn fiber contour. Now click M to measure the end-to-end length.
    6. Repeat the same procedure on at least 10 fibrils per image.
    7. Collect those two measurements from each of 10 fibrils and input the data into an excel spreadsheet, expressing total fiber length (contour) and end-to-end length (straight connecting line) as Length [curve] and Length [linear], respectively.
    8. Calculate the waviness index (W) using the formula: W= Length [curve]/ Length [linear].
    9. Calculate the % of waviness comparing data from the images of treated samples(SMG) with the images from control samples using the formula: (W[SMG] - 1) / (W[control] - 1)

10. Perform a pairwise t-test for waviness index (W) in order to determine statistical differences (p-values) of collagen fiber morphology between different treatment conditions and control.

Representative Results

Thermal denaturation temperature (Tm) as an assay method to evaluate TXL cross-linking effect: A total of 16 pairs of rabbit eyes were used in these experiments for the TXL procedure.As an initial part of this study, the localization of cross-linking effect induced by a single injection of SMG cross-linking agent via sT space in the cadaveric rabbit head was evaluated. This type of experiment has relevance to the clinical treatment of patients, since injections in more than one location could be necessary to stabilize a desired area of sclera.

As would be predicted based on basic diffusivity principles, the effect was greatest at the site of injection with effects induced in adjacent regions as well, depending on the concentration of the solutions. **Figure 1A** represents the schematic location of scleral sectors (1-4 in red hollow number font) (further divided into squares (1-16 in black thin number font)) that underwent separate thermal denaturation analysis following a single sT injection with color mapping index. **Table 1** shows the change in Tm values for each numbered sector as compared to its corresponding control. Values are included for both 40 mM and 400 mM injections and include standard error of the mean calculated for a minimum of three independent determinations.

Figures 1B-C represent the results using two different concentrations of SMG, 40 mM (**Figure 1B**) and 400 mM (**Figure 1C**). In **Figure 1B**, the lower concentration 40 mM sample showed a mild shift in Tm which was noted in square 2 (the injection site). Similar shifts were seen in adjacent squares 1 and 3 (lighter blue). Marginal shifts are seen in squares 4 to 6 and 7 to 9 without statistically significant differences from the injected square. No Tm shift was seen in the lower squares 14 to 16, which represented the most distant sector away from the injection site.

As shown in **Figure 1C**, the higher concentration (400 mM) had a statistically highly significant cross-linking effect (indicated as shades of orange). A large shift in Tm with associated small standard deviation and $p< 0.05$ were observed, reflecting a large difference in the effect of the 400 mM compared to lower 40 mM concentration. The most dramatic effects were noted in sector 1 in the upper globe. With regard to the remaining sectors, a lesser effect was observed in squares 10 and 14 (which may have been due to some tracking of cross-linking fluid posteriorly) and no effect was observed in squares 11, 12, 13, 15, and 16. Overall, the cross-linking effects were marginal in sectors 2 and 3 with no effect observed in sector 4 (*i.e.*, the most distant location from the injection site), similar to the 40 mM sample. These results indicated that there was a "zone of effect" and that this type of pattern could be expected following a sT injection of cross-linking agent. This could indicate the need for injection in several locations in order to induce effects over a wide area of tissue.

Study of the cross-linking effects induced in intact eyes evaluating TXL with two concentrations of SMG was also performed. Thermal denaturation analysis of tissue that underwent such scleral cross-linking was performed. Cross-linking time was 3.5 h for TXL using three different concentrations, 40 (Tm=1.11+/-1.2), 100 (Tm=5.12+/-2.9), and 400 (Tm=14.34+/-1.1) mM SMG. The results showed that there is a concentration dependent effect seen in SMG cross-linked tissue.

Second harmonic generation (SHG) imaging as a method to evaluate TXL cross-linking effect:

SHG microscopy images were analyzed both for pixel intensity of the SHG signal and fiber bundle waviness. A wide span of cross-linking concentrations (from 40 to 400 mM) was used in order to explore the SHG signal changes that may occur over a wide range of cross-linking effects. Using the histogram analysis capability included in the Fiji image processing program[20], it was possible to quantitate the SHG signal produced in scleral tissue by sT injection, comparing the effects at 40 mM to those induced using 400 mM. The average difference in mean pixel intesities at 40 mM were 66.3 ± 27.7 compared to 361.4 ± 28.3 for the 400 mM samples, a nearly 6-fold increase. This corresponds with an increase in tissue cross-linking, since corresponding increases in Tm also were noted under these conditions. **Figure 2** shows representative SHG images of sclera taken from control (**Figure 2A**), 40 mM (**Figure 2B**), and 400 mM (**Figure 2C**). The accompanying histogram analysis, including mean brightness (or pixel intensity) is also shown. The total number of images analyzed was: 120 for 40 mM and 98 for its control; 121 for 400 mM and 94 for its own control. The depth of tissue imaging was 10 to 15 µm from the episcleral surface. The results of the histogram analyses, which involved the averaging of numerous image fields, indicated that higher concentrations of cross-linking effect **(Figure 3)** produced greater pixel intensities.

As shown in **Figure 4**, an image analysis was also performed with methods adopted from the cardiovascular blood vessel literature, using the ImageJ plugin "*Neuron J*"[21]. We estimated the waviness factor W=Length[curve]/Length[linear] and we observed that cross-linking resulted in straightening of fiber bundles as indicated by a decreased waviness % in 40 mM and 400 mM cross-linked sclera versus untreated control sclera (W%=(W[SMG]-1)/(W[control]-1), **Table 2**). The difference in waviness between 40 and 400 mM SMG treated samples was not statistically significant.

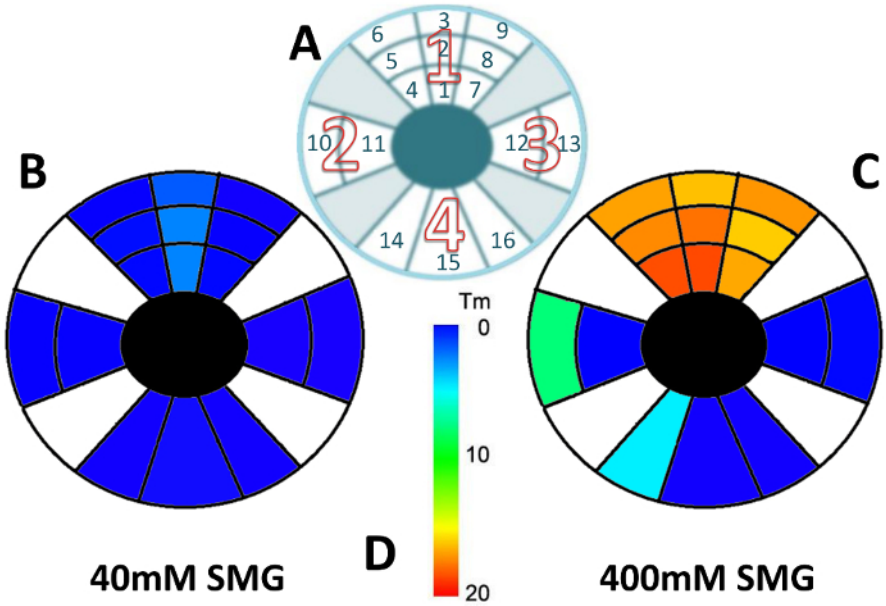

Figure 1: Localization of TXL effect via sT injection using 40 and 400 mM SMG.
(A) Schematic representation of 4 scleral sectors (numbers 1-4 in large red hollow font), with sclera divided into squares [numbers 1-16 in smaller black thin font] (not drawn to scale) that underwent thermal analysis. The injection site corresponded to the centrally located square (square 2) in sector 1. The thermal denaturation cross-linking effect of TXL with **(1B)** 40 mM SMG and **(1C)** 400mM SMG. **(D)** Color coded temperature scale legend for **(B)** and **(C)**. This figure has been modified from Zyablitskaya *et al.* with permission[22]. Please click here to view a larger version of this figure.

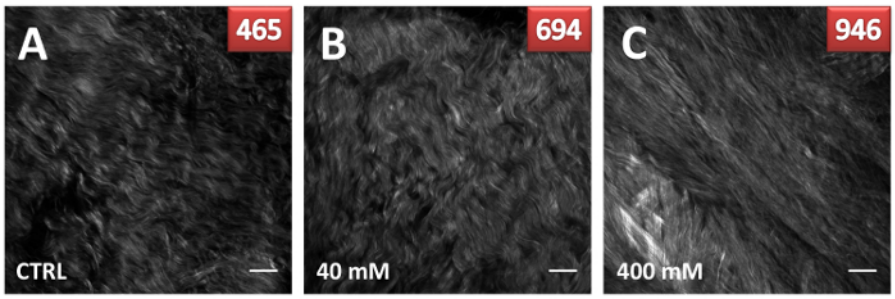

Figure 2: Representative images of concentration dependent increases in SHG signal brightness levels produced following TXL using SMG via sT injection of sclera *ex vivo*. Concentrations of SMG are shown as **(B)** 40mM and **(C)** 400mM. Each image contains a 50 µm scale bar (right lower corner) and mean pixel intensity value (right upper corner) - absolute values. This figure has been modified from Zyablitskaya *et al.* with permission[22]. Please click here to view a larger version of this figure.

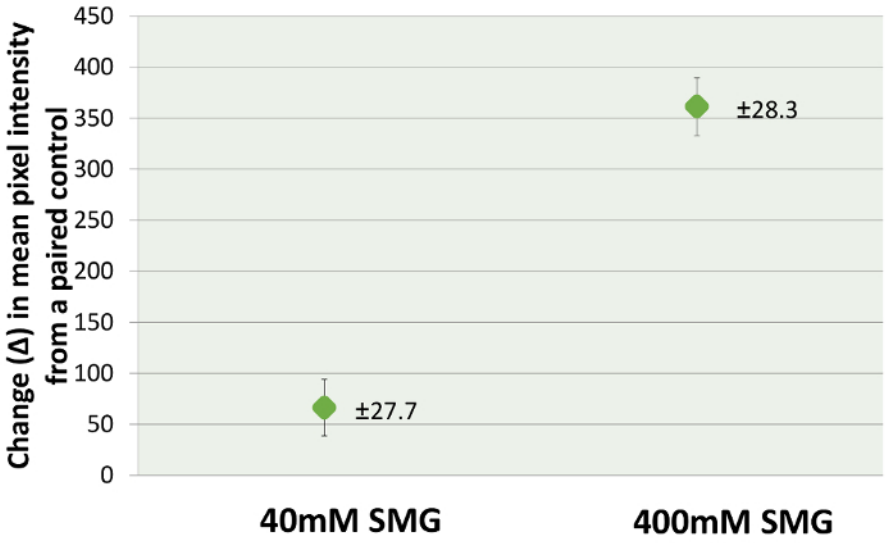

Figure 3: Bar chart of the change (Δ) in SHG signal pixel intensity (as compared to a paired control from the same rabbit head) in scleral intact globes cross-linked via sT injection (TXL) with 40 and 400 mM SMG solutions. Average values with standard error of the mean were: 66 ± 27.7 for 40 mM and 361 ± 28.3 for 400 mM. This figure has been modified from Zyablitskaya *et al.* with permission[22]. Please click here to view a larger version of this figure.

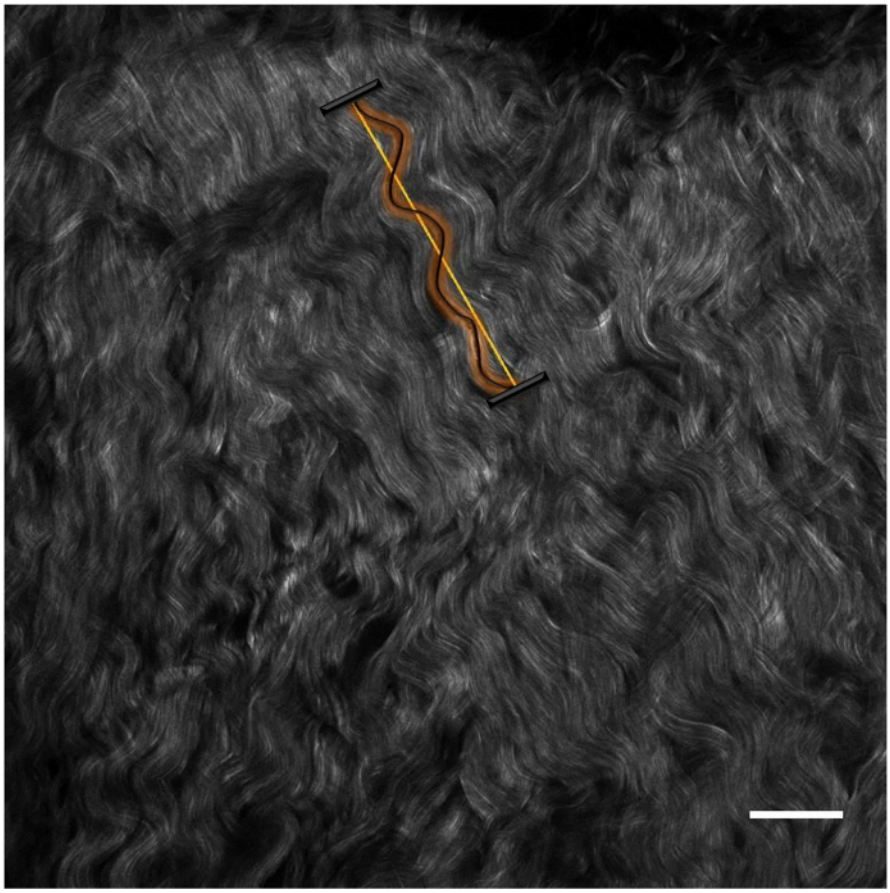

Figure 4: Example of fiber waviness analysis (as expressed by linearity). Image of control sample for 40 mM SMG concentration with a 50 µm scale bar (right lower corner). This figure has been modified from Zyablitskaya *et al*. with permission[22]. Please click here to view a larger version of this figure.

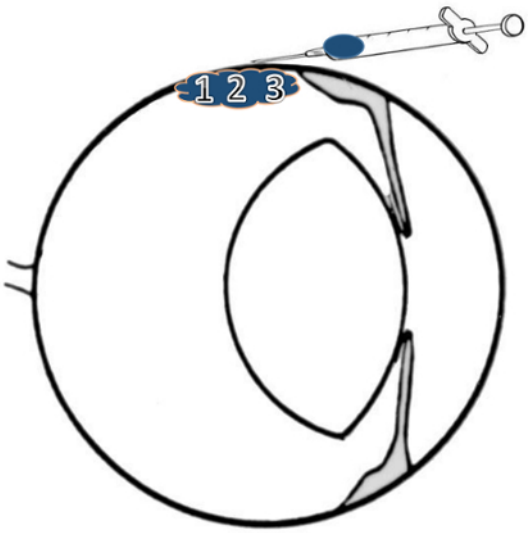

Figure 5: Schematic representation of sT injection. Areas numbered 1-3 correspond to areas represented in the **Figure 1A**. Please click here to view a larger version of this figure.

	±Δ Tm	
area	40mM	400mM
1	3.4 ±2.8	20.5 ±0.6
2	3.4 ±0.53	19.58 ±1.5
3	2.5 ±2.47	17.99 ±3.06
4	0.72 ±0.9	20.36 ±0.19
5	0.85 ±0.55	19.11 ±1.33
6	0.52 ±1.35	18.66 ±4.1
7	0.78 ±1.6	18.44 ±2.8
8	0.56 ±0.9	17.77 ±2.69
9	0.22 ±0.6	18.92 ±2.6
10	0.46 ±0	8.75 ±10.56
11	0.47 ±0.18	0.63 ±1.84
12	0.11 ±0.08	0.66 ±1.52
13	0.08 ±0.05	0.71 ±2.17
14	0.22 ±0.7	5.71 ±0.29
15	0.32 ±0.2	0.29 ±0.7
16	0.24 ±0.73	0.26 ±0.79

Table 1: DSC results for localization of TXL effect study. Change in thermal melting temperatures (ΔTm) with standard errors for each sampled sector is as depicted in **Figure 1A**. Each value is expressed as the difference in Tm ascompared to its paired control and is an average of a minimum of 3 independent determinations.

SMG, mM	Waviness	Waviness-%	t-test vs. [0 mM SMG]
0	1.106 ± 0.044	100	
40	1.067 ± 0.017	63	$p < 0.02$
400	1.059 ± 0.009	55	$p < 0.003$
Linear fibers	1.000	0	
(Theoretical)			

Table 2. Results of fiber waviness analysis. SHG images from the area of TXL injection were analyzed for degree of fiber waviness using Neuron J software. Ten fibers were selected from each image and a total of approximately 100 fibers were analyzed for degree of waviness. Average values with standard error of the mean are included.

Discussion

Conducted experiments have shown evidence supporting the use of SHG signal microscopy as a method for evaluation of collagen cross-linking effects in sclera, raising the future possibility of using this technique as a monitoring tool for cross-linking treatments that target collagen proteins. Of note, an instrument already is in clinical use that can potentially capture this SHG signal. Although this instrument was primarily designed for imaging skin human dermis, it has been used successfully to image cornea and sclera[23].

It is necessary to maintain identical scanning and imaging conditions when comparing control and treated samples. Second harmonic generation microscopy of collagen in sclera tissue requires a fluorescence microscope compatible with multi-photon imaging, a pulsed infrared laser tunable in the 800-900 nm wavelength range, and a highly sensitive detector such as the GaAsP non-descanned (NDD) detectors. Guidelines described in this manuscript are a starting point. The conditions should be determined specifically for the new experiments or for the different systems.

The cornea and sclera also have been evaluated concurrently in studies using this technique[24,25,26,27]. Knowing that the SHG signal propagates in both forward and backward directions, several studies have examined corneal tissue independently in its native state[28,29,30,31,32,33,34] and in keratoconus[35,36] as well as following CXL (as discussed below). The results of these studies indicate that the corneal signal is optimized in the forward scattered direction, which makes sense given the cornea's transparency and the fact that light passes through the tissue to strike a monitor in forward scattered systems. Typically, the SHG signal is in the blue visible range and will be greatly reduced when passing through a highly scattering tissue like the eye sclera. As a result, detection of the forward scattered SHG would require a thin section of tissue of 50 µm or less in thickness, as well as a special optical set-up. In contrast, the back-scattered signal can be captured through the regular light path of a fluorescence microscope without tissue sectioning and therefore this mode is preferred when imaging collagen in intact sclera tissue to a depth of 30-40 µm. In this study, we noted a concentration dependent increase in signal density. It is quite possible, however, that the TXL might have had additional and similar effects on deeper layers of the sclera, and that the effect could be more pronounced and extend to deeper layers particularly with the higher concentration. However, due to the limited SHG signal penetration in the sclera and for the purposes of this initial study, we chose to work with the best quality images, which were obtained from the most superficial sclera (15 µm depth). In future studies, we will consider depth dependent effects following TXL methods as this may provide additional important information as to why even greater differences were not observed between 40 and 400 mM treated samples.

Furthermore, regarding the use of SHG for evaluating riboflavin CXL induced tissue cross-linking, SHG microscopy imaging following riboflavin CXL of the cornea have been reported by several groups[37,38,39,40,41]. In a study by Steven *et al.*[37], corneal stabilization using the CXL technique resulted in a "homogenization" of signal and loss of tissue "folds" or "undulations" seen in non-cross-linked samples. These types of changes, however, also were noted in a study evaluating the effects of changes in IOP on corneal SHG signals, raising the possibility of technical artefacts. Organizationally from the fibril as well as the higher order fiber bundle/lamellar organization standpoint, the sclera and cornea are quite different and much is known about such differences from electron microscopy studies.The two tissues differ with regard to fibril packing, which includes fibril diameter distribution (small uniform fibrils for the cornea and variable diameter fibrils for the sclera) and inter-fibril spacing (uniform for cornea and variable for sclera). As well, the higher order organization into lamellar sheets (cornea) versus fiber bundles (sclera) is quite different. Such structural differences are reflected in the SHG signals produced by these two tissues. Thus, changes induced by cross-linking may alter the SHG signal in different but parallel ways. In other words, the "straightening" of fibers in the sclera observed in this study, and the "homogenization" of signal in the cornea reported in the literature, were both the result of collagen cross-linking modification. Thus, the "homogenization" effect in the cornea could in some way be analogous to the "straightening" effect of the sclera that has been reported here.

The mechanisms that result in this straightening effect produced by TXL are unclear based on the current study. One possibility could be that the tissue was somehow "fixed" in a mechanically "loaded" position.This would support the notion that induced "fibril and fiber stabilization" had occurred. Changes in intraocular pressure likely did not contribute to this effect since IOP was monitored prior to and following the sT injection and remained stable. Overall, the significance of these observations are unclear and further studies will be necessary. Of note, separate imaging techniques such as Brillouin microscopy[42], which has been shown to provide quantitative measures of cross-linking (as determined by shear modulus) following CXL photochemistry may be useful in confirming the findings with SHG imaging in this study. However, it should be noted that its use with highly scattering tissues such as the sclera[43], requires technical modifications and has not been validated with cross-linked scleral tissue.

Laser polarization and SHG microscopy is an important issue. The laser light is linearly polarized and oriented perpendicular to the direction of SHG signal propagation and at some angle in the xy-plane to each collagen fiber. Thus, fibers in the xy-plane that are well aligned and exactly perpendicular to the polarized laser light will produce a higher SHG signal than those at other angles, including those parallel to the incident light (*i.e.*, z-plane), which will produce the lowest SHG signal (due to destructive interference). With respect to sclera tissue, collagen fibers are oriented at various angles on a microscopic level, although preferred anatomic fiber orientations are known to exist based on globe location. Thus, since the SHG signal produced will vary depending on the xy-plane angle of each fiber, the overall signal will be less than that which would be produced if all the collagen fibers were exactly aligned at the same angle (in a tissue such as a tendon, for example). Thus, in this study, due to the nature of the sample being imaged, the direction of polarization was not intentionally determined but was kept consistent throughout the study. Furthermore, we took care to obtain tissues from treated and control globes from identical scleral regions, minimizing any differences in fiber orientation between samples. Finally, we analyzed over 100 images per sample in order to obtain intensity values. This extensive evaluation should have normalized any aberrant SHG signals that may have been registered. That being said, it is possible that as a result of the "fiber straightening" that we observed in the cross-linked samples (described above), a greater proportion of "in focal plane" fibers could have contributed to the increase in the SHG signal as well as increased SHG signals from greater xy-plane alignment. Both of these possibilities would be manifestations of induced cross-linking effects.

A regional analysis of cross-linking changes (by Tm) induced by an sT injection of SMG was performed. As expected, the level of cross-linking effect was concentrated in the area of the injection. Little or no cross-linking effect was noted in the region directly opposite (furthest away) from the injection, consistent with what is known regarding localization of effect following sT injection as shown by ultrasound localization[44,45] and computed tomography[46].

Finally, regarding cross-linking therapy and myopia, collagen cross-linking of the cornea is finding widespread use in the treatment of corneal destabilization including keratoconus, post LASIK keratectasias, pellucid marginal degeneration (PMD), and as an adjunct to refractive surgical procedures[47]. The success of treating corneal disease with cross-linking has led to the exploration of applying this treatment approach to the back of the eye and, in particular, the sclera, for limiting axial elongation in high myopia[2], a concept that goes back to the very earliest stages of the therapeutic cross-linking concept[48,49].

Disclosures

The authors have nothing to disclose.

Acknowledgements

The authors thank Tongalp Tezel, MD, for consultation regarding sT injection; Theresa Swayne, PhD, for consultation regarding SHG microscopy; and Jimmy Duong from the Design and Biostatistics Resource and the Biostatistical core facility of the Irving Institute at Columbia University Medical Center.

Supported in part by Research to Prevent Blindness and by National Institutes of Health Grants NCRR UL1RR024156, NEI P30 EY019007, NCI P30 CA013696, and NEI R01EY020495 (DCP). Columbia University owns related intellectual property: US issued patents no: 8,466,203 and no: 9,125,856. International patent pending: PCT/US2015/020276.

Images were collected in the Confocal and Specialized Microscopy Shared Resource of the Herbert Irving Comprehensive Cancer Center at Columbia University, supported by NIH grant #P30 CA013696 (National Cancer Institute). The confocal microscope was purchased with NIH grant #S10 RR025686.

References

1. McBrien, N. A., & Norton, T. T. Prevention of collagen crosslinking increases form-deprivation myopia in tree shrew. *Exp Eye Res.* **59** (4), 475-486 (1994).
2. Elsheikh, A., & Phillips, J. R. Is scleral cross-linking a feasible treatment for myopia control? *Ophthalmic Physiol Opt.* **33** (3), 385-389 (2013).
3. Dotan, A. *et al.* Scleral cross-linking using riboflavin and ultraviolet-a radiation for prevention of progressive myopia in a rabbit model. *Exp Eye Res.* **127** 190-195 (2014).
4. Canavan, K. S., Dark, A., & Garrioch, M. A. Sub-Tenon's administration of local anaesthetic: a review of the technique. *Br J Anaesth.* **90** (6), 787-793 (2003).
5. Guise, P. Sub-Tenon's anesthesia: an update. *Local Reg Anesth.* **5** 35-46 (2012).
6. Ahn, J. S. *et al.* A sub-Tenon's capsule injection of lidocaine induces extraocular muscle akinesia and mydriasis in dogs. *Vet J.* **196** (1), 103-108 (2013).
7. Wollensak, G., & Redl, B. Gel electrophoretic analysis of corneal collagen after photodynamic cross-linking treatment. *Cornea.* **27** (3), 353-356 (2008).
8. Liu, T. X., & Wang, Z. Collagen crosslinking of porcine sclera using genipin. *Acta Ophthalmol.* **91** (4), e253-257 (2013).
9. Wang, M., & Corpuz, C. C. Effects of scleral cross-linking using genipin on the process of form-deprivation myopia in the guinea pig: a randomized controlled experimental study. *BMC Ophthalmol.* **15** 89 (2015).
10. Babar, N. *et al.* Cosmetic preservatives as therapeutic corneal and scleral tissue cross-linking agents. *Invest Ophthalmol Vis Sci.* **56** (2), 1274-1282 (2015).
11. Kim, S. Y. *et al.* Evaluating the Toxicity/Fixation Balance for Corneal Cross-Linking With Sodium Hydroxymethylglycinate (SMG) and Riboflavin-UVA (CXL) in an Ex Vivo Rabbit Model Using Confocal Laser Scanning Fluorescence Microscopy. *Cornea.* **35** (4), 550-556 (2016).
12. da Cruz, L. G. I., Moraes, G. d. A., Nogueira, R. F., Morandim-Giannetti, A. d. A., & Bersanetti, P. A. DSC characterization of rabbit corneas treated with Stryphnodendron adstringens (Mart.) Coville extracts. *Journal of Thermal Analysis and Calorimetry.* (2017).
13. Bersanetti, P. A. *et al.* Characterization of Rabbit Corneas Subjected to Stromal Stiffening by the Acai Extract (Euterpe oleracea). *Curr Eye Res.* **42** (4), 528-533 (2017).
14. Freund, I., & Deutsch, M. Second-harmonic microscopy of biological tissue. *Opt Lett.* **11** (2), 94 (1986).
15. Campagnola, P. J., & Loew, L. M. Second-harmonic imaging microscopy for visualizing biomolecular arrays in cells, tissues and organisms. *Nat Biotechnol.* **21** (11), 1356-1360 (2003).
16. Williams, R. M., Zipfel, W. R., & Webb, W. W. Interpreting second-harmonic generation images of collagen I fibrils. *Biophys J.* **88** (2), 1377-1386 (2005).
17. Mansfield, J. *et al.* The elastin network: its relationship with collagen and cells in articular cartilage as visualized by multiphoton microscopy. *J Anat.* **215** (6), 682-691 (2009).
18. Tsamis, A., Krawiec, J. T., & Vorp, D. A. Elastin and collagen fibre microstructure of the human aorta in ageing and disease: a review. *J R Soc Interface.* **10** (83), 20121004 (2013).
19. Raub, C. B. *et al.* Noninvasive assessment of collagen gel microstructure and mechanics using multiphoton microscopy. *Biophys J.* **92** (6), 2212-2222 (2007).
20. Schindelin, J. *et al.* Fiji: an open-source platform for biological-image analysis. *Nat Methods.* **9** (7), 676-682 (2012).
21. Meijering, E. *et al.* Design and validation of a tool for neurite tracing and analysis in fluorescence microscopy images. *Cytometry A.* **58** (2), 167-176 (2004).
22. Zyablitskaya, M. *et al.* Evaluation of Therapeutic Tissue Crosslinking (TXL) for Myopia Using Second Harmonic Generation Signal Microscopy in Rabbit Sclera. *Invest Ophthalmol Vis Sci.* **58** (1), 21-29 (2017).
23. Steven, P., Muller, M., Koop, N., Rose, C., & Huttmann, G. Comparison of Cornea Module and DermaInspect for noninvasive imaging of ocular surface pathologies. *J Biomed Opt.* **14** (6), 064040 (2009).

24. Han, M., Giese, G., & Bille, J. F. Second harmonic generation imaging of collagen fibrils in cornea and sclera. *Optics Express.* **13** (15), 5791-5797 10.1364/Opex.13.005791, (2005).
25. Wang, B. G., Konig, K., & Halbhuber, K. J. Two-photon microscopy of deep intravital tissues and its merits in clinical research. *J Microsc.* **238** (1), 1-20 (2010).
26. Teng, S. W. *et al.* Multiphoton autofluorescence and second-harmonic generation imaging of the ex vivo porcine eye. *Invest Ophthalmol Vis Sci.* **47** (3), 1216-1224 (2006).
27. Rao, R. A., Mehta, M. R., Leithem, S., & Toussaint, K. C., Jr. Quantitative analysis of forward and backward second-harmonic images of collagen fibers using Fourier transform second-harmonic-generation microscopy. *Opt Lett.* **34** (24), 3779-3781 (2009).
28. Morishige, N., Petroll, W. M., Nishida, T., Kenney, M. C., & Jester, J. V. Noninvasive corneal stromal collagen imaging using two-photon-generated second-harmonic signals. *J Cataract Refract Surg.* **32** (11), 1784-1791 (2006).
29. Aptel, F. *et al.* Multimodal nonlinear imaging of the human cornea. *Invest Ophthalmol Vis Sci.* **51** (5), 2459-2465 (2010).
30. Winkler, M. *et al.* Nonlinear optical macroscopic assessment of 3-D corneal collagen organization and axial biomechanics. *Invest Ophthalmol Vis Sci.* **52** (12), 8818-8827 (2011).
31. Morishige, N., Takagi, Y., Chikama, T., Takahara, A., & Nishida, T. Three-dimensional analysis of collagen lamellae in the anterior stroma of the human cornea visualized by second harmonic generation imaging microscopy. *Invest Ophthalmol Vis Sci.* **52** (2), 911-915 (2011).
32. Gore, D. M. *et al.* Two-photon fluorescence microscopy of corneal riboflavin absorption. *Invest Ophthalmol Vis Sci.* **55** (4), 2476-2481 (2014).
33. Park, C. Y., Lee, J. K., & Chuck, R. S. Second Harmonic Generation Imaging Analysis of Collagen Arrangement in Human Cornea. *Invest Ophthalmol Vis Sci.* **56** (9), 5622-5629 (2015).
34. Quantock, A. J. *et al.* From nano to macro: studying the hierarchical structure of the corneal extracellular matrix. *Exp Eye Res.* **133** 81-99 (2015).
35. Morishige, N. *et al.* Quantitative analysis of collagen lamellae in the normal and keratoconic human cornea by second harmonic generation imaging microscopy. *Invest Ophthalmol Vis Sci.* **55** (12), 8377-8385 (2014).
36. Morishige, N. *et al.* Second-harmonic imaging microscopy of normal human and keratoconus cornea. *Invest Ophthalmol Vis Sci.* **48** (3), 1087-1094 (2007).
37. Steven, P., Hovakimyan, M., Guthoff, R. F., Huttmann, G., & Stachs, O. Imaging corneal crosslinking by autofluorescence 2-photon microscopy, second harmonic generation, and fluorescence lifetime measurements. *J Cataract Refract Surg.* **36** (12), 2150-2159 (2010).
38. Bueno, J. M. *et al.* Multiphoton microscopy of ex vivo corneas after collagen cross-linking. *Invest Ophthalmol Vis Sci.* **52** (8), 5325-5331 (2011).
39. McQuaid, R., Li, J. J., Cummings, A., Mrochen, M., & Vohnsen, B. Second-Harmonic Reflection Imaging of Normal and Accelerated Corneal Crosslinking Using Porcine Corneas and the Role of Intraocular Pressure. *Cornea.* **33** (2), 125-130 (2014).
40. Laggner, M. *et al.* Correlation Between Multimodal Microscopy, Tissue Morphology, and Enzymatic Resistance in Riboflavin-UVA Cross-Linked Human Corneas. *Invest Ophthalmol Vis Sci.* **56** (6), 3584-3592 (2015).
41. Chai, D. *et al.* Quantitative assessment of UVA-riboflavin corneal cross-linking using nonlinear optical microscopy. *Invest Ophthalmol Vis Sci.* **52** (7), 4231-4238 (2011).
42. Scarcelli, G. *et al.* Brillouin microscopy of collagen crosslinking: noncontact depth-dependent analysis of corneal elastic modulus. *Invest Ophthalmol Vis Sci.* **54** (2), 1418-1425 (2013).
43. Shao, P., Besner, S., Zhang, J., Scarcelli, G., & Yun, S. H. Etalon filters for Brillouin microscopy of highly scattering tissues. *Opt Express.* **24** (19), 22232-22238 (2016).
44. Kumar, C. M., & McNeela, B. J. Ultrasonic localization of anaesthetic fluid using sub-Tenon's cannulae of three different lengths. *Eye (Lond).* **17** (9), 1003-1007 (2003).
45. Winder, S., Walker, S. B., & Atta, H. R. Ultrasonic localization of anesthetic fluid in sub-Tenon's, peribulbar, and retrobulbar techniques. *J Cataract Refract Surg.* **25** (1), 56-59 (1999).
46. Ripart, J., & Eledjam, J. J. [Locoregional anesthesia for ophthalmic surgery: unique episcleral injection (sub-tenon) in the internal canthus]. *Ann Fr Anesth Reanim.* **17** (4), Fi72-74 (1998).
47. Meek, K. M., & Hayes, S. Corneal cross-linking--a review. *Ophthalmic Physiol Opt.* **33** (2), 78-93 (2013).
48. Wollensak, G., & Spoerl, E. Collagen crosslinking of human and porcine sclera. *J Cataract Refract Surg.* **30** (3), 689-695 (2004).
49. Paik, D. C., Wen, Q., Airiani, S., Braunstein, R. E., & Trokel, S. L. Aliphatic beta-nitro alcohols for non-enzymatic collagen cross-linking of scleral tissue. *Exp Eye Res.* **87** (3), 279-285 (2008).

